



Fatigue and creep to leak tests of proton exchange membranes using pressure-loaded blisters

Yongqiang Li^{a,*}, David A. Dillard^a, Scott W. Case^a, Michael W. Ellis^b,
Yeh-Hung Lai^c, Craig S. Gittleman^c, Daniel P. Miller^c

^a Department of Engineering Science and Mechanics, Virginia Polytechnic Institute and State University, Blacksburg, VA 24061-0219, United States

^b Department of Mechanical Engineering, Virginia Polytechnic Institute and State University, Blacksburg, VA 24061-0238, United States

^c Fuel Cell Research Lab, GM R&D, General Motors Corporation, 10 Carriage Street, Honeoye Falls, NY 14472-0603, United States

ARTICLE INFO

Article history:

Received 8 April 2009

Received in revised form 15 June 2009

Accepted 15 June 2009

Available online 2 July 2009

Keywords:

Proton exchange membrane

Mechanical durability

Fatigue

Creep

Gas crossover

Pressure-loaded blister

ABSTRACT

In this study, three commercially available proton exchange membranes (PEMs) are biaxially tested using pressure-loaded blisters to characterize their resistance to gas leakage under either static (creep) or cyclic fatigue loading. The pressurizing medium, air, is directly used for leak detection. These tests are believed to be more relevant to fuel cell applications than quasi-static uniaxial tensile-to-rupture tests because of the use of biaxial cyclic and sustained loading and the use of gas leakage as the failure criterion. They also have advantages over relative humidity cycling test, in which a bare PEM or catalyst coated membrane is clamped with gas diffusion media and flow field plates and subjected to cyclic changes in relative humidity, because of the flexibility in allowing controlled mechanical loading and accelerated testing. Nafion[®] NRE-211 membranes are tested at three different temperatures and the time–temperature superposition principle is used to construct stress–lifetime master curve. Tested at 90 °C, 2%RH extruded Ion Power[®] N111-IP membranes have a longer lifetime than Gore[™]-Select[®] 57 and Nafion[®] NRE-211 membranes.

© 2009 Elsevier B.V. All rights reserved.

1. Introduction

Among many obstacles that proton exchange membrane fuel cells face before more widespread usage in automotive applications is the need for improved and quantifiable durability of fuel cell stack components [1]. Mechanical durability issues of the proton exchange membrane or polymer electrolyte membrane (PEM) or membrane electrode assembly (MEA) as a whole include, but may not be limited to, pinholes through the membrane leading to reactant gas crossover and buckling of the membrane that causes delamination at the catalyst/membrane interface [2,3]. A wide range of studies addressing mechanical issues of membranes have emerged in the last few years. These studies mostly fall into three basic categories: (1) constitutive properties of free standing membranes [4–15], (2) numerical stress analysis of subgasket- or diffusion media- and bipolar plates-constrained membranes [11,15–20], and (3) strength or endurance testing of free standing membranes using controlled loading frames [8–11,21–24].

This study focuses on characterizing the lifetime of PEMs under both cyclic and sustained mechanical loading. Automotive fuel cell stacks can be subjected to frequent start–stop cycles and cycles due to variation in the power demand from the driver. To evaluate the mechanical durability of PEMs under cyclic or sustained mechanical stresses due to these operating requirements, the relative humidity (RH) cycling test has become a routine screening test [2,3,9,15,20,25], in which a bare PEM or catalyst coated membrane is clamped between gas diffusion media and flow field plates and subjected to cyclic changes in relative humidity in the flow field. Differential air pressure is periodically applied to measure the leakage over the entire active area and the test is terminated when the leakage exceeds a certain threshold. Practically, limited by the diffusion kinetics of water in the membrane, each RH cycle between saturation ($\lambda > 14$) and dry ($\lambda < 3$) conditions often takes several minutes. Because stresses induced in the membrane solely by cycling the RH are often small, RH cycling tests can become very time-consuming and expensive as more and more durable membranes are developed. It is difficult to quantify the hygral stress history in the membrane during RH cycling tests because both the hygral strains and the constitutive properties of the membrane are highly dependent on time, moisture content, and temperature. A result of this is that the applied stresses in RH cycling tests cannot be easily controlled. When devising ex situ mechanical testing methods, it is desirable to conduct fatigue or creep to leak tests of

* Corresponding author. Present address: Fuel Cell Research Lab, GM R&D, General Motors Corporation, 10 Carriage Street, Honeoye Falls, NY 14472-0603, United States. Tel.: +1 585 624 6560; fax: +1 585 624 6680.

E-mail address: li233@vt.edu (Y. Li).

Nomenclature

a	radius
a_T	thermal shift factor
a_H	hygral shift factor
B_0	coefficient in Hencky's series solution
E	relaxation modulus or Young's Modulus
E_i	coefficients in Prony series
E_∞	equilibrium modulus in Prony series
h	membrane thickness
i	natural number
n	number of terms in Prony series
p	pressure
r	radial coordinate
t	time
t_f	failure time
T	temperature

Greek symbols

λ	number of water molecules per SO_3^- in proton exchange membranes
ν	Poisson's ratio
σ	stress
τ_i	relaxation time in Prony series
θ	circumferential coordinate

PEMs at controlled and increased stress levels without altering the failure mode.

Before focusing on a particular experimental technique, it is worthwhile to examine a few unique features of fatigue or creep to leak tests of PEMs. Because of their viscoelastic nature, fatigue failure of polymers is often exacerbated by thermal softening and is highly dependent on the frequency of cycling [26]. Being extremely thin, PEMs may be studied more easily in that any heat generated during cycling may be easily released into the environment. Fatigue tests of structural materials can start with as-received specimens to study the initiation of fatigue cracks and subsequent failure, or with specimens containing sharp precracks to study fatigue crack propagation under prescribed cyclic changes in a fracture parameter such as stress intensity factor or strain energy release rate. For PEMs, crack propagation through the thickness is of primary interest from a gas crossover perspective. In reality, sharp cracks may readily form in the catalyst layers or at the catalyst–PEM interface, but in ex situ fatigue test of bare PEMs, it is not easy to introduce a sharp precrack in the thickness direction because of the small thickness and the significant ductility of the membranes. Readers may well consider ex situ fatigue testing of cracked catalyst coated membranes (CCM), but we do not deem such tests relevant. The primary reason is that in a fuel cell the CCM is constrained from in-plane straining while in an ex situ test, in all likelihood, one need apply stresses and stretch the CCM, therefore the effect of the cracks in the catalyst layers on the membrane durability are different. Secondly, before these cracks can be well quantified and controlled in manufacturing, ex situ tests of CCMs only lead to data of limited applicability. In fatigue failure of structural polymeric materials, crazes or microfatigue cracks often precedes the formation of cracks of catastrophic size [26]. Therefore, the failure criterion for characterizing PEMs should not be complete rupture of the specimen, as is typically characterized in uniaxial tensile tests, since it is evident that crazes or cracks may be sufficient to allow gas leakage before developing into catastrophic ruptures.

Following the above reasoning, pressure-loaded blister tests appear to be well suited for ex situ fatigue or creep to leak (instead of complete rupture) tests of PEMs in that they enable easy control

over cyclic or sustained loading and lend themselves to convenient detection of gas leakage. In an earlier paper, we discussed the use of blister specimens to characterize the biaxial burst strength of PEMs and listed some advantages of blister specimens for testing PEMs [23]. Among them, a few relevant to fatigue and creep to leak tests are presented here along with additional insights provided by the unique features of fatigue testing of PEMs conducted in the manner discussed above. In the blister burst test [23], the equal biaxial stress state induced within the central region of the pressurized blister simulates the biaxial stress state within a PEM fuel cell, where the membrane is constrained from in-plane straining and the hygrothermal stresses of primary interest are inherently biaxial. The fact that the in-plane stress components within the blisters achieve their maxima at the center of the blister and decrease toward the edge effectively reduces the chance of grip failures, which is frequently seen in uniaxial tests of straight-sided thin polymer membrane specimens. At the same time, such stress distribution in the blister helps reduce the chance of failure related to defects introduced during the preparation of specimens, since in contrast to cutting a uniaxial tensile test specimen, the blister test specimens are cut well away from where failure will occur (details of sample preparation will be discussed in the Section 2). Since our interest is in the membrane's capability of containing gas, the pressure of the loading medium, air, can be directly used to detect leakage. Once there is a connected pathway for air to leak across the membrane, should it be a crack or craze, a pressure drop will be observed. The pressure-loaded blister configuration easily links cycle- and time-dependent testing to the failure criterion most relevant to fuel cell applications.

2. Experimental technique

In [23], using individual Swagelok® (Swagelok Company, Solon, OH) tube fittings, the authors reported the use of pressure-loaded blisters for quasi-static biaxial strength test of PEMs. In the present study, a multi-cell fixture was fabricated to clamp multiple specimens in a similar fashion for testing under fatigue and creep to leak loading conditions.

The concept of loading a thin film specimen using a pressure-loaded blister is illustrated in Fig. 1(a), in which the specimen is clamped around the edge and allowed to deflect into a blister (or bulge) through a circular opening of diameter $2a$ when loaded with air pressure, p , from one side. The circular shape and the size of the blister are just chosen for the purpose of applying the biaxial stresses and readers are urged not to imagine blisters of the same geometry must exist in operating fuel cells for the present testing method to be relevant. An analysis relating the biaxial stresses in the membrane, the applied air pressure and the geometry of the blister is given in Section 3. Practically, the clamping method used in the present study is schematically shown in Fig. 1(b). The radius at the bottom of the conical opening in the stainless steel (SS) top plate and that in the PTFE washer are both 9.53 mm. Pressurized air can be fed from the hole in the bottom plate to pressurize the specimen. The PTFE washer and the backing sheet on the bottom plate were used to enhance gripping as well as to facilitate removal of the failed membrane, which would otherwise stick to the SS plates after long periods of testing at elevated temperatures. A fixture that includes eight individual cells is pictured in Fig. 1(c), in which opaque Gore™ Select®-57 (Gore-57, W.L. Gore & Associates, Newark, DE) specimens were used for clarity. Two such fixtures were enclosed side by side in a Cincinnati Sub-Zero (Cincinnati Sub-Zero Products, Inc., Cincinnati, OH) humidity chamber, allowing a total of sixteen specimens to be tested together.

A schematic diagram of the pressure control apparatus used to generate cyclic and sustained pressure histories is illustrated in Fig. 2. In the center of the diagram is the test fixture (shown in

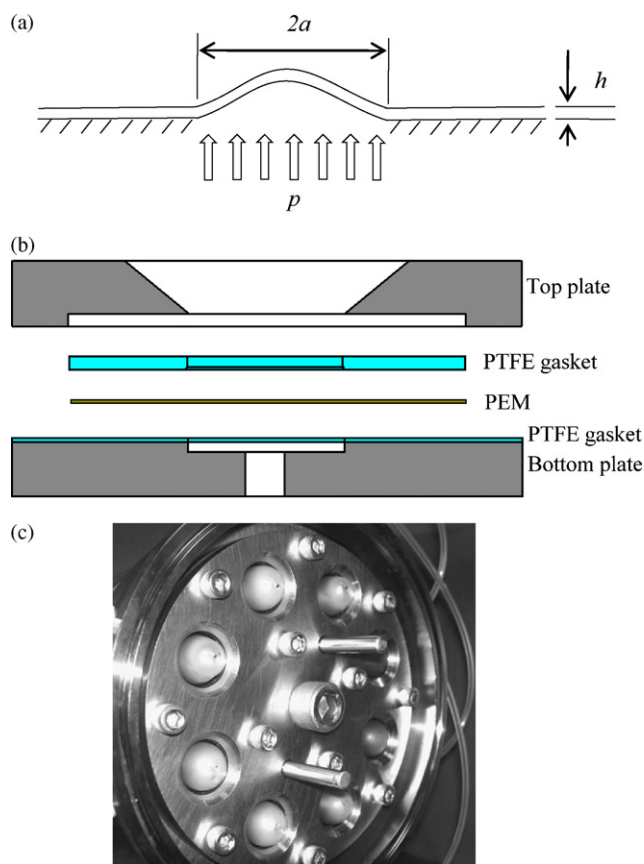


Fig. 1. (a) The concept of a pressure-loaded blister; (b) a schematic of an individual cell of the fixture photographed in (c), which is a photo of a test in progress.

Fig. 1(c)) holding eight blisters. The eight specimens were separated into two groups, each of which was fed with pressurized air from one of the two air reservoirs. The air reservoirs were supplied with shop air and pressures in them were controlled using two Tescom® (Tescom Corporation, Elk River, MN) current-to-pressure controllers (model ER3000). Individual solenoid valves were used to either connect each blister specimen to the associated reservoir for pressurization or to atmosphere for venting. Needle valves (Swagelok® SS-SS2-VH) with maximum flow coefficient of 0.004 installed between the solenoid valves and the blisters were used to limit the flow rate of air coming into each blister during normal operation. The needle valve setting helped define a threshold leaking rate as the failure criterion based on the pressure drop in the blister when there was a leak. In this study, a 15% drop of pressure measured by the pressure sensor next to the blister from the pressure level in the air reservoir was chosen as the failure criterion. For example, assuming a test pressure of 30 kPa, the flow coefficient of 0.004 and the pressure drop of 4.5 kPa across the needle valve means a threshold leaking rate of 380 sccm; if the test pressure is 10 kPa, the threshold leaking rate is 204 sccm.

In a creep to leak test of a group of four blisters, the solenoid valves kept the blisters connected with one of the reservoirs. In a fatigue test of a group of four blisters, the solenoid valves cyclically switched between the reservoir and the atmosphere. When there was detectable leakage at any blister in the group, the corresponding valve switched the leaking blister to the atmosphere so that testing of the rest of the group was not interrupted. The control process was executed with a LabView® (National Instruments, Inc., Austin, TX) VI, which also recorded the pressure in each blister every 2 s.

As an example, the pressure history during the last ten cycles in the lifetime of a blister specimen is shown in Fig. 3. As can be seen in the figure, in each cycle, the blister was pressurized for 10 s and then vented to atmosphere for 4 s. The 10-s hold gave reasonable time for the pressure in the blister to stabilize. If the loading period had been adjusted to 2 s, a triangular waveform would have been generated rather than a near-square waveform. In the last cycle, when the failure criterion of a 15% pressure drop from the pressure set point was met, the pressure supply was cut off and the preceding cycle was counted as the number of fatigue life cycles. This number, multiplied by 10 s, gives the net time under loading, which will be used as a metric of lifetime for fatigue failure. It can be seen that in this particular test the leakage developed rather suddenly and the blister completely ruptured as the leakage developed. At lower pressure levels, the blisters often fail by gradual development of leakage and never completely rupture.

Three commercially available PEMs were tested in this study, namely Nafion® NRE-211 (E. I. du Pont de Nemours and Company, Wilmington, DE), Gore™ Select Series®-57 (Gore-57) and Ion Power N111-IP (Ion Power, Inc., New Castle, DE). They are nominally 25 μm, 18 μm, and 25 μm thick, respectively. The NRE-211 membrane is a cast homogeneous perfluorosulfonic acid (PFSA) membrane [27]. The Gore-57 membrane has three layers, including the central reinforcing layer consisting of a composite network of expanded polytetrafluoroethylene (e-PTFE) and PFSA fillers, and the outer PFSA layers [28]. The N111-IP membrane is an extruded version of NRE-211 [29]. In wet (2 min) to dry (2 min) RH cycling tests ($\lambda > 14$ to $\lambda < 3$) at 80 °C without electrochemical loading, NRE-211 had the shortest lifetime (~4000 cycles), followed by Gore-57 with some slight improvement (~6000 cycles), and N111-IP, which had a significantly longer RH cycling lifetime (>20,000 cycles) [25].

For each set of testing, sixteen square pieces of PEM with an edge length of 25 mm were cut with a razor blade in ambient laboratory conditions of 23 °C and 30%RH. Because of the PEMs' tendency to adhere to the PTFE gasket on the bottom plate, the samples were able to be smoothly laid flat and clamped onto the fixtures in the environmental chamber which was then heated to the desired test temperature and RH level. Small hygrothermal stresses may develop in the PEM because of this change of environment, but should relax to a negligible level after an hour of equilibration in the chamber (as will be explained in Section 3 based on the viscoelastic nature of the membranes). However, the presence of this stress may be representative of actual stack conditions as fuel cells are typically assembled in room conditions.

Creep to leak tests of all three membranes were conducted at 90 °C, 2%RH. Fatigue to leak tests of NRE-211 membranes were conducted at three temperatures, 70 °C, 80 °C and 90 °C, all at 2%RH. Fatigue to leak tests of N111-IP and Gore-57 were conducted at 90 °C, 2%RH. There were several reasons for choosing these test conditions. The temperature range addressed is representative of the harsher operating condition seen in operating fuel cells. As PEMs in operating fuel cells are subjected to the highest tensile stresses during a wet to dry cycle, it makes sense to obtain the resistance to leak under dry condition. Although the probability of achieving "bone dry" condition is low, it is reasonable to use the dry condition to accelerate ex situ testing. Recently, there have been reports that the mechanical behaviors of PEMs under extremely dry conditions may be so significantly different from wetter conditions that time-temperature-humidity superposition may not be applicable [6,13]. Therefore, the focus of this paper is on illustrating the potential of the testing method and for completeness tests under elevated RH conditions have been planned for future studies. Finally, as mentioned in the previous paragraph, the samples were clamped at 23 °C and 30%RH, drying the membrane to nearly a dry state at elevated temperatures helped keep the membrane taut before testing.

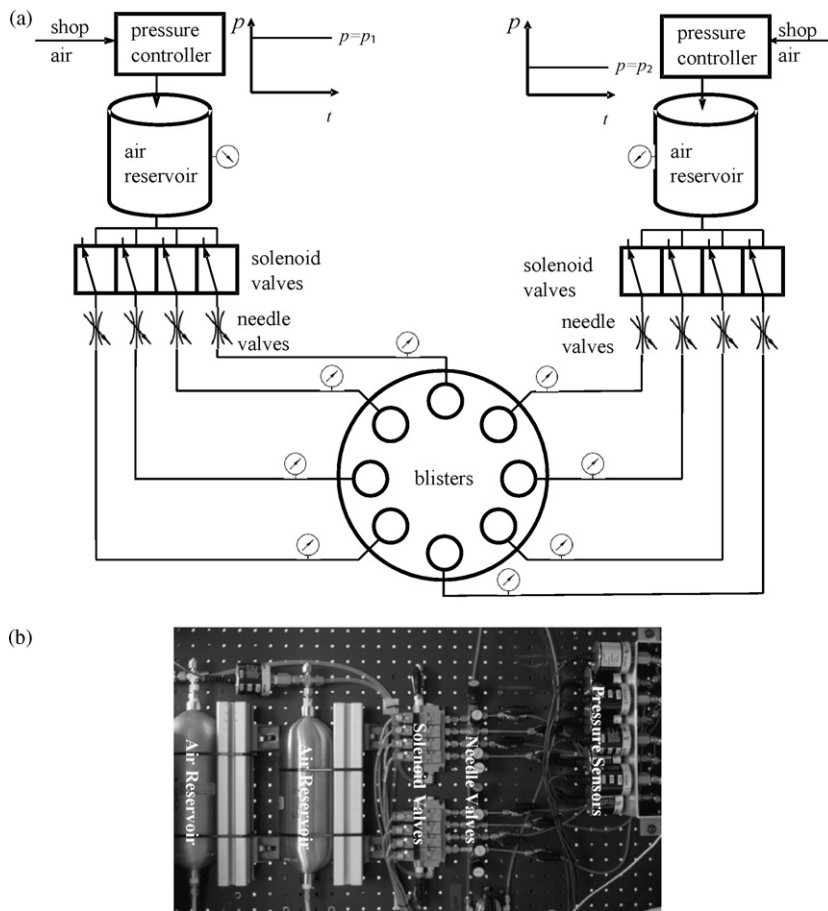


Fig. 2. (a) Schematic diagram of the multi-specimen test fixture and pressurization apparatus; (b) a picture showing two air reservoirs on the left, two groups of solenoid valves in the middle and eight pressure sensors on the right that monitor the pressure histories in the blisters.

3. Analysis

A key step in the analysis of the experimental results is converting the lateral pressure into the biaxial stress at the center of the blister. To this end, Hencky’s solution for a circumferentially clamped isotropic linear elastic membrane subjected to lateral pressure [30] was employed, in conjunction with the quasi-elastic approximation for simple assessment of stresses in viscoelastic materials [31]. According to Hencky’s solution, the maximum radial and circumferential stress components in a pressure-loaded circular blister appear in the center of the blister and can be expressed

as:

$$\sigma_r = \sigma_\theta = \frac{B_0}{4} \left(\frac{Ep^2 a^2}{h^2} \right)^{1/3}$$

resulting in an equal biaxial stress state at the center of the blister. It should be noted that the coefficient B_0 is mildly dependent on the Poisson’s ratio, which is not constant for a viscoelastic material. However, within the possible range of the Poisson’s ratio of PEMs, 0.35–0.50, B_0 only changes from 1.748 to 1.845 [23]. Based on a published Poisson’s ratio of NRE-211 (0.4 [19]), B_0 used in the following calculation is 1.777.

According to the quasi-elastic approximation, which states that the solution for a linear viscoelastic boundary value problem for nearly constant stress (or strain) histories, the strain (or stress) can be calculated by simply replacing the elastic compliance (or modulus) with the creep compliance (or the stress relaxation modulus) in the linear elastic solution [31], the stress at the time of failure at the center of a blister loaded with constant pressure is expressed as:¹

$$\sigma_r(t_f) = \sigma_\theta(t_f) = \frac{B_0}{4} \left(\frac{E(t_f)p^2 a^2}{h^2} \right)^{1/3}$$

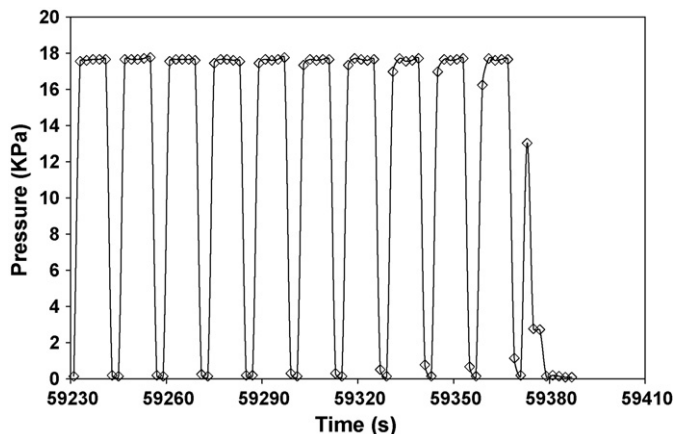


Fig. 3. The pressure history during the last ten cycles in a typical fatigue test.

¹ In the case of pressure-loaded blisters, neither the strain nor stress in the blister remains perfectly constant over time. Another version of the equation is to use creep compliance $1/D(t_f)$ in place of $E(t_f)$.

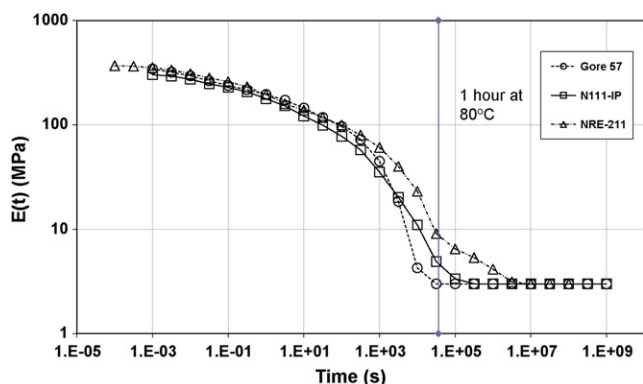


Fig. 4. The relaxation moduli of the three membranes as approximated with respective Prony series [12,13].

The quasi-elastic approximation is usually good when the loading is a step function, which is the case for the constant pressure tests. At this time, the quasi-elastic approximation was also used for calculating the stress at failure for the fatigue tests using the net time under pressure. This approximation is crude, but is a first step before more sophisticated means such as finite element models that account for the large deformation occurring in the blister and more viscoelastic properties of the PEMs become available. Preliminary FEM analysis based on linear viscoelastic material properties indicate that substantial thinning in the membrane can occur and the true stress in the blister can be much larger than the quasi-elastic approximation, which essentially gives the engineering stress by assuming a constant membrane thickness. The relaxation modulus master curves of the three membranes, shown in Fig. 4 referenced at 70 °C and 30%RH, can be expressed with a Prony series of the form [32]:

$$E(t) = E_{\infty} + \sum_{i=1}^n E_i e^{-t/\tau_i}$$

The E_{∞} 's, E_i 's, and τ_i 's for the three membranes are tabulated in Tables 1–3, all referenced at 70 °C and 30%RH, obtained with stress relaxation tests as described in Refs. [12,13]. It should be noted that the rubbery plateau modulus value of 3 MPa for all three membranes were assumed values, based on the trends shown in the relaxation moduli curves and the understanding of typical amorphous polymers above their α transition temperatures [32]. This assumption may not be true for the Gore-57 membrane, which has a reinforcement layer in the center. Given $E(t)$ at 70 °C and 30%RH, in order to calculate stresses at a different pair of temperature and RH values, hygrothermal shift factors must be used following the time–temperature–moisture superposition principle to find the

Table 1
Prony series parameters of NRE-211.

$E_{\infty} = 3 \text{ MPa}$		
i	$E_i \text{ (MPa)}$	τ_i
1	19.0	1.0E–03
2	60.8	1.0E–02
3	36.5	1.0E–01
4	86.6	1.0E+00
5	40.8	1.0E+01
6	36.3	1.0E+02
7	41.1	1.0E+03
8	41.2	1.0E+04
9	1.8	1.0E+05
10	3.1	1.0E+06

Table 2
Prony series parameters of Gore-57.

$E_{\infty} = 3 \text{ MPa}$		
i	$E_i \text{ (MPa)}$	τ_i
1	33.2	1.26E–03
2	38.0	9.09E–03
3	37.0	3.03E–02
4	24.7	1.09E–01
5	25.5	4.76E–01
6	23.8	1.92E+00
7	54.7	1.02E+01
8	30.5	7.39E+01
9	34.7	4.24E+02
10	26.3	1.55E+03
11	34.2	3.01E+03

Table 3
Prony series parameters of N111-IP.

$E_{\infty} = 3 \text{ MPa}$		
i	$E_i \text{ (MPa)}$	τ_i
1	55.0	1.26E–02
2	15.0	6.54E–02
3	53.8	4.97E–01
4	63.8	5.41E+00
5	40.5	5.90E+01
6	50.2	6.43E+02
7	21.1	7.39E+03
8	3.2	4.60E+04

corresponding modulus [32], i.e.:

$$E_{T,RH}(t) = E_{70^{\circ}\text{C}, 30\%RH} \left(\frac{t}{a_T a_H} \right)$$

The logarithmic shift factors, $\log_{10}(a_T)$ and $\log_{10}(a_H)$ used for the three membranes are tabulated in Table 4. The vertical line in Fig. 4 represents an equivalent time of 1 h at 80 °C, indicating that the residual tensile stress due to the environmental change from sample preparation (23 °C, 30%RH) to testing (80 °C, 2%RH) after the 1 h equilibration process is negligible:

$$\begin{aligned} \sigma &= - \frac{E(\alpha\Delta T + \beta\Delta\lambda)}{1 - \nu} \\ &= - \frac{10 \text{ MPa} \times (0.000123 \times 57 - 0.01 \times 2)}{1 - 0.4} \approx 0.2 \text{ MPa}. \end{aligned}$$

When strength vs. lifetime curves are obtained at different conditions, the time–temperature–humidity superposition principle can be used again to construct a master curve of strength at reference temperature and RH levels using the same shift factors. The same procedure has been successful in processing PEM blister burst results obtained at different temperatures [24] and PEM fracture energy results obtained at different temperatures and humidity levels [22]. Again, it should be noted here and following that behaviors of PEMs under extremely low RH can deviate from behaviors

Table 4
Logarithmic shift factors obtained with uniaxial tensile stress relaxation test^a.

T (°C)	NRE-211	Gore-57	N111-IP
70	0	0	0
80	–1	–	–
90	–2.2	–0.9	–1.4
RH%	NRE-211	Gore-57	N111-IP
2	0.1	0.1	0.1
30	0	0	0

^a As no tests were done at 80 °C for Gore-57 and N111-IP, no temperature shift factors were used (dashes in the table).

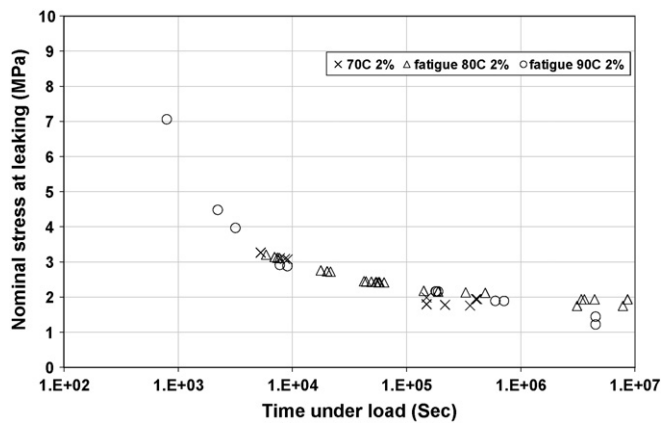


Fig. 5. The fatigue results of NRE-211 at three temperatures. The 70 °C and 90 °C data were shifted to the reference temperature 80 °C (using shift factors obtained from stress relaxation tests) according to the time–temperature superposition principle.

at moderate or high RH. Before more understandings on such differences are gained and more tests at elevated humidities are conducted, we caution readers not to make excessive extrapolation of the data reported here from tests run under extremely dry condition.

4. Results and discussion

The results from fatigue tests of NRE-211 at 70 °C, 80 °C, and 90 °C, all at 2%RH are shown together in Fig. 5. The 70 °C and 90 °C results were shifted to 80 °C and 2%RH using the temperature shift factors (obtained with uniaxial tensile stress relaxation tests) shown in Table 4. It is seen that the data from the three different conditions can be superimposed, or in other words, the acceleration of testing time by raising the temperature can be explained by the viscoelastic properties of the membranes. Of particular note is that the shift factors obtained from stress relaxation tests are appropriate for forming a fatigue life master curve for the Nafion® NRE-211 membranes, evidence of the appropriateness of shift factors for predicting other material response [32].

The trend shown by the data follows typical fatigue lifetime curves. The lifetime curves may be partitioned into a crack formation-dominated zone (high stress level) and a crack propagation-dominated zone (low stress level). The fatigue strength decreases sharply at high stress levels and then more slowly as the applied stress level is decreased. The sharp decrease at high stress levels may be due to crazes or cracks formation within the first few cycles; at low stress levels the time required to initiate crazes or cracks in the membrane becomes highly sensitive on the stress applied [26].

The fatigue and creep to leak results of the three membranes at 90 °C and 2%RH are shown in Figs. 6 and 7. Clear differences among the three membranes are seen from these plots. At high stress levels, NRE-211 is inferior to both Gore-57 and N111-IP; N111-IP has a longer lifetime than the other two over the entire stress range. A separation is seen between the Gore-57 membrane and the NRE-211 membrane at high stress levels (larger than around 2.5 MPa), but not at low stress levels. This may mean that the reinforcement layer restricted early craze or crack formation in the membrane, but is less effective in the crack propagation-dominated lower stress levels. Plotted on the same scale, it seems that with the current fatigue cycling pattern (10 s with pressure and 4 s without pressure), the fatigue and creep to leak results are almost identical and no clear cyclic effect can be found. In other words, the lifetime under load appears to be predominantly determined by viscoelastic behavior of the membrane rather than cyclic loading, in that it

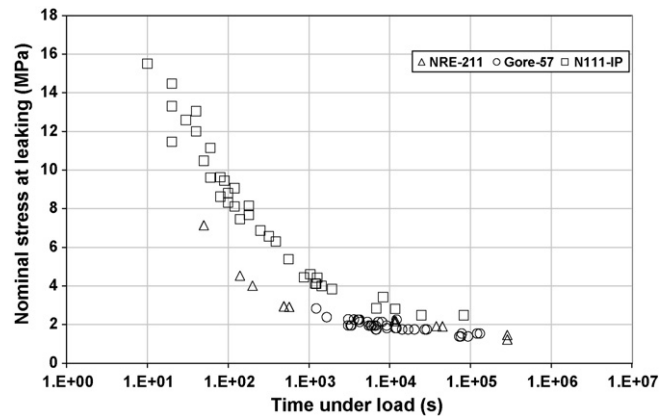


Fig. 6. The fatigue results of the three membranes at 90 °C.

is the time at load rather than the number of cycles that appears important.

Several encouraging facts are seen from these results. From the NRE-211 tests conducted at different temperatures the time–temperature superposition principle using shift factors obtained from relaxation tests seems to work well, so should be useful for accelerated testing. The longest fatigue and creep to leak tests of all three membranes conducted at 90 °C lasted around four days, except for a few creep to leak tests. This method produces leak failures much quicker than RH cycling tests at 80 °C (for example, the N111-IP membrane can last more than 20,000 4 min 0–150%RH cycles, which takes around 56 days). Considering the stresses present during RH cycling tests [33] in conjunction with these fatigue and creep to leak resistance results, the ranking of these three membranes in terms of RH cycling lifetime can be easily understood: NRE-211 faced the worst situation with the maximum hygral stress coupled with the lowest resistance to fatigue and creep damage; Gore®-57 and N111-IP experience similar amounts of hygral stress during RH cycling, but the inferior resistance to fatigue and creep loading shown by Gore-57 leads to its shorter lifetime than N111-IP during RH cycling test. These two observations (the accelerating and the ranking capabilities) plus the ease of quickly obtaining large quantities of useful lifetime data by testing multiple samples under controlled environmental conditions warrant wide use of the pressure-loaded blister fatigue and creep test method for screening PEMs for automotive fuel cell applications.

The pressure-loaded blister test is not without shortcomings, however. In these ex situ tests, only in-plane stresses are considered, whereas in fuel cell stacks, the compressive stress in the thickness

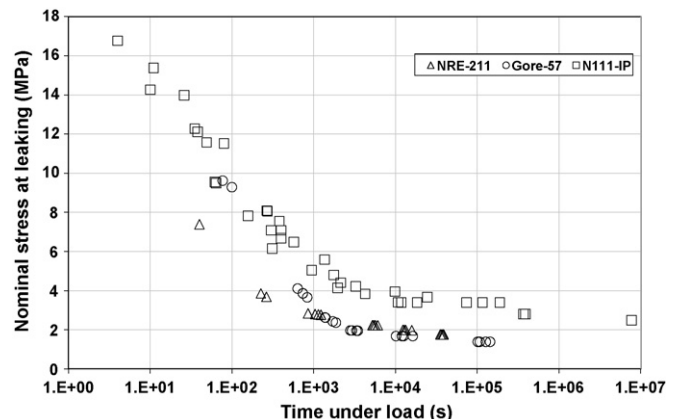


Fig. 7. The creep to leak results of the three membranes at 90 °C.

direction of the PEM can also lead to deformation that assists the onset of gas crossover. Compressive stresses are included in situ RH cycling tests but are not included in either conventional uniaxial tensile tests or the biaxial blister test reported herein.

In comparison to uniaxial tensile tests in which the (engineering) stress in the membrane is directly known, the stresses in the pressure-loaded blister tests must be calculated from the air pressure history, geometric parameters, and constitutive properties of the membranes. Exact determination would require extensive knowledge in the constitutive properties of the membrane. As the properties of the membrane continuously change because of its viscoelastic nature, even though the amplitude of the air pressure remains constant, the evolution of stresses in the membrane may be complicated. Many fuel cell membranes are not isotropic in-plane, which requires stress analysis more involved than the Hencky's equation. To close this gap, studies are underway including experimental measurement of the deflection of the membrane during the test and finite element stress analysis.

In this study and other ex situ tests found in the literature, no electrochemical effect was introduced, while in reality electrochemical and mechanical effects can interact and accelerate each other. Furthermore, electron microscope images may be used to investigate whether the failure mechanisms during the blister tests, the RH cycling tests and during the practical operation of a fuel cell are the same.

5. Conclusions

The mechanical durability of proton exchange membranes is essential for building robust and long-lasting PEM fuel cells for automotive applications. In this study, pressure-loaded blisters have been used to test PEMs in a manner that successfully overcomes several issues associated with quasi-static uniaxial tensile strength tests and RH cycling tests. By controlling the air pressure, cyclic and sustained loading can be applied to the membrane and at cyclic frequencies considerably higher than allowed in RH cycling tests. As a result of its circular geometry, equal biaxial stresses occur in the center of the blister and the stress components gradually decreases toward the edge of the blister, reducing the likelihood of edge or grip failure. The air used to pressurize the membrane can be readily used for leak detection. As higher stresses can be applied on the membrane during these tests than during RH cycling tests, the testing time can be significantly reduced especially as more durable membranes become available. For the materials tested herein, a similar ranking in lifetime were achieved with mechanical pressurization tests in less than 10% of the time required for RH cycling tests.

Fatigue and creep to leak results obtained for NRE-211 at 70 °C, 80 °C and 90 °C, all at 2%RH were used to form a lifetime master curve by shifting according to the time–temperature–humidity superposition principle using shift factors obtained with uniaxial tensile relaxation tests. This indicates that the development of gas crossover passages through the thickness of the membrane is controlled by the intrinsic viscoelastic processes in the membrane. This observation is consistent with the fracture test reported in [22] and ramp to burst test of pressure-loaded blisters reported in [24]. Comparison between the three commercial membranes shows the same ranking in terms of resistance to fatigue and creep loadings as that obtained with the RH cycling test, that the extruded N111-IP is more durable than the cast NRE-211 and the reinforced Gore-57 lifetime is intermediate but closer to NRE-211 [25]. A closer examination at the lifetime data of N111-IP and Gore-57 seems to indicate that the reinforcement in Gore-57 was beneficial only at high stress levels. No clear evidence of cyclic effect was found when comparing the fatigue and creep to leak results, suggesting that time at load is of prime importance. Further studies will focus on obtaining more

experiment data at elevated humidities to better simulate the operating conditions in a fuel cell and experimental and numerical stress analyses to gain more understandings on the stress evolution in the blister during long term/cyclic testing as well as the effect of anisotropy in the membrane.

Acknowledgment

The authors would like to thank General Motors Corporation for supporting this research.

References

- [1] U.S. Department of Energy, Office of Basic Energy Sciences. "Basic Research Trends for the Hydrogen Economy", US DOE, Washington, DC, 2004.
- [2] W. Liu, K. Ruth, G. Rusch, J. New Mater. Electrochem. Syst. 4 (2001) 227–231.
- [3] Y.-H. Lai, D.A. Dillard, in: W. Vielstich, H.A. Gaistager, H. Yokokawa (Eds.), Handbook of Fuel Cells, vol. 5, John Wiley and Sons, New York, 2009.
- [4] J.T. Uan-Zo Li, The effects of structure, humidity and aging on the mechanical properties of polymeric ionomers for fuel cell applications Master Thesis, Virginia Polytechnic Institute and State University, Blacksburg, VA, 2001.
- [5] D.E. Curtin, R.D. Lousenberg, T.J. Henry, P.C. Tangeman, M.E. Tisack, J. Power Sources 131 (2004) 41–48.
- [6] F. Bauer, S. Denebler, M. Willert-Porada, J. Polym. Sci. Part B: Polym. Phys. 43 (2005) 786–795.
- [7] S. Kundu, L.C. Simon, M. Fowler, S. Grot, Polymer 46 (2005) 11707–11715.
- [8] D. Liu, S. Kyriakides, S.W. Case, J.J. Lesko, Y.X. Li, J.E. McGrath, J. Polym. Sci. Part B: Polym. Phys. 44 (2006) 1453–1465.
- [9] X.Y. Huang, R. Solasi, Y. Zou, M. Feshler, K. Reifsnider, D. Condit, S. Burlatsky, T.T. Madden, J. Polym. Sci. Part B: Polym. Phys. 44 (2006) 2346–2357.
- [10] Y. Tang, A.M. Karlsson, M.H. Santare, M. Gilbert, S. Cleghorn, W.B. Johnson, Mater. Sci. Eng. A 425 (2006) 297–304.
- [11] Y. Tang, A. Kusoglu, A.M. Karlsson, M.H. Santare, S. Cleghorn, W.B. Johnson, J. Power Sources 175 (2008) 817–825.
- [12] K.A. Patankar, D.A. Dillard, S.W. Case, M.W. Ellis, Y.-H. Lai, M.K. Budinski, C.S. Gittleman, Mech. Time Depend. Mater. 12 (2008) 221–236.
- [13] K.A. Patankar, D.A. Dillard, S.W. Case, M.W. Ellis, Y.-H. Lai, M.K. Budinski, C.S. Gittleman, J. Membr. Sci., in review.
- [14] M. B. Satterfield, Mechanical and water sorption properties of Nafion and composite Nafion/titanium dioxide membranes for polymer electrolyte membrane fuel cells, Ph.D. dissertation, Princeton University, Princeton, NJ, 2008.
- [15] Y.-H. Lai, C.S. Gittleman, C.K. Mittelsteadt, D.A. Dillard, Proceedings of the 3rd International Conference on Fuel Cell Science, Engineering and Technology, Ypsilanti, MI, 2005.
- [16] Y. Tang, M.H. Santare, A.M. Karlsson, S. Cleghorn, W.B. Johnson, J. Fuel Cell Sci. Technol. 3 (2006) 119–124.
- [17] M.A.R.S. Al-Baghdadi, H.A.K.S. Al-Janabi, Energy Fuels 21 (2007) 2258–2267.
- [18] A. Kusoglu, A.M. Karlsson, M.H. Santare, S. Cleghorn, W.B. Johnson, J. Power Sources 170 (2007) 345–358.
- [19] R. Solasi, Y. Zou, X.Y. Huang, K. Reifsnider, D. Condit, J. Power Sources 167 (2007) 366–377.
- [20] Y.-H. Lai, C.K. Mittelsteadt, C.S. Gittleman, D.A. Dillard, J. Fuel Cell Sci. Technol. 6 (2009) 021002–021014.
- [21] D.A. Dillard, M.K. Budinski, Y.-H. Lai, C.S. Gittleman, Proceedings of the 3rd International Conference on Fuel Cell Science, Engineering and Technology, Ypsilanti, MI, 2005.
- [22] Y. Li, J.K. Quincy, S.W. Case, M.W. Ellis, D.A. Dillard, Y.-H. Lai, M.K. Budinski, C.S. Gittleman, J. Power Sources 185 (2008) 374–380.
- [23] D.A. Dillard, Y. Li, J.R. Grohs, S.W. Case, M.W. Ellis, Y.-H. Lai, M.K. Budinski, C.S. Gittleman, J. Fuel Cell Sci. Technol. 6 (2009) 031014–031021.
- [24] J.R. Grohs, Y. Li, D.A. Dillard, S.W. Case, M.W. Ellis, Y.-H. Lai, M.K. Budinski, C.S. Gittleman, J. Power Sources, in review.
- [25] C.S. Gittleman, Y.-H. Lai, D.P. Miller, Extended Abstract, the AIChE 2005 Annual Meeting, Cincinnati, OH, 2005.
- [26] R.W. Hertzberg, J.A. Manson, Fatigue of Engineering Plastics, Academic Press, New York, 1980.
- [27] DuPont Fuel Cells, Dupont Nafion PFSA membranes: NRE-211 and NRE-212, available at: <http://www.fuelcell.com/techsheets/Nafion%20NRE-211%20212.pdf>.
- [28] J.A. Kolde, B. Bahar, M.S. Wilson, T.A. Zawodzinski, S. Gottesfeld, Proceedings of the 1st International Symposium on Proton Conducting Membrane Fuel Cells, Chicago, IL, 1995.
- [29] Ion Power, Inc., Product information, available at: <http://www.ion-power.com/products.html#films>.
- [30] H. Hencky, Z. Math. Phys. 63 (1915) 311–317.
- [31] J.D. Murff, R.A. Schapery, Int. J. Numer. Anal. Methods Geomech. 10 (1986) 449–458.
- [32] J.D. Ferry, Viscoelastic Properties of Polymers, Wiley, New York, 1980.
- [33] Y. Li, D.A. Dillard, S.W. Case, M.W. Ellis, Y.-H. Lai, C.S. Gittleman, Exp. Mech., in review.